Journal of Materials Chemistry C

Accepted Manuscript

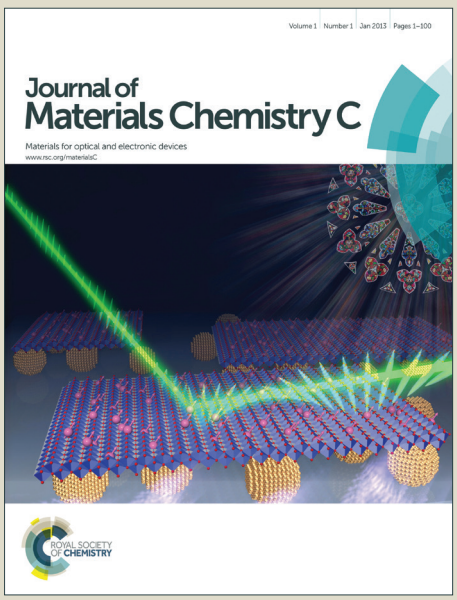

ROYAL SOCIETY OF CHEMISTRY

www.rsc.org/materialsC

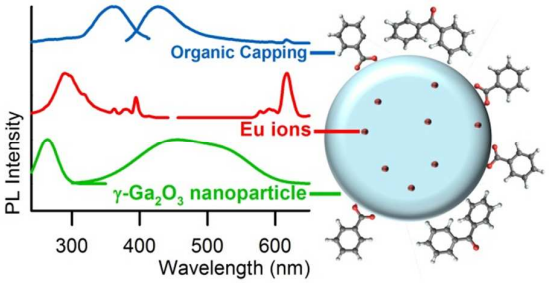

Pure and Eu-doped γ-Ga_2O_3 nanopowders with organic capping layer were obtained by benzyl alcohol route.

Photoluminescence experiments allow to assign the strong blue light emission to aromatic ketone derivative.

Cite this: DOI: 10.1039/c0xx00000x

www.rsc.org/xxxxxx

ARTICLE TYPE

Non-aqueous sol-gel synthesis of hybrid rare-earth doped γ-Ga_2O_3 nanoparticles with multiple organic-inorganic-ionic light-emission features

Roberto Lorenzi[a*], Alberto Paleari[a,b], Nikita V. Golubev[b], Elena S. Ignat'eva[b], Vladimir N. Sigaev[b], Markus Niederberger[c], Alessandro Lauria[c*]

Received (in XXX, XXX) Xth XXXXXXXXX 20XX, Accepted Xth XXXXXXXXX 20XX
DOI: 10.1039/b000000x

We present a novel strategy for the synthesis of pure and Eu-doped γ-Ga_2O_3 nanoparticles (NP) with organic *in situ* capping resulting from a non-aqueous solution-based benzyl alcohol route. Photoluminescence spectroscopy points out concomitant benzoate-related and γ-Ga_2O_3 exciton-like Eu^{3+} excitation in the UV, and blue emission – superimposed to γ-Ga_2O_3 donor-acceptor recombination – ascribable to organic moieties different from benzoate.

Gallium sesquioxide (Ga_2O_3) is a wide band gap material (~4.9 eV) currently used in semiconductor industry mainly as target for deposition of thin film transistor for next-generation flat-panel displays. Bulky and nanostructured Ga_2O_3 have also been deeply investigated as luminescent materials,[1] insulating barrier in magnetic tunnel junctions,[2] and active substrate for sensoristic and photocatalysis.[3] The majority of these studies consider only the most stable form of Ga_2O_3, that is the monoclinic β phase, although Ga_2O_3 exists in five different polymorphs: α, β, γ, δ, and ε.[4] Indeed, the metastable cubic γ phase presents several fascinating properties that may be crucial for further applications. The synthesis routes and the preparation of γ-Ga_2O_3 are either chemical, physical or biochemical reactions. It has been produced in form of colloids or nanopowders through sol-gel derived synthesis,[5] thin films through the pulsed laser deposition,[6] elongated platelets through enzymatic synthesis,[7] and nanoparticles embedded in glass through secondary phase transformation.[8] All the reported syntheses bring to nano- or micro-sized phases with very large surface area and high crystal defectiveness. Large surface area is expected to improve catalytic and sensor performances, while the presence of localized hole and electron traps (i.e. cation and/or oxygen vacancies) is crucial in photonic and optoelectronic applications. In fact, the intense blue emission at around 460 nm – excited by band-to-band transitions and quite ubiquitous in gallium oxide compounds – is the result of radiative recombination of donor and acceptor pairs (DAPs). In these oxides, DAPs are formed by an oxygen vacancy $V_O^{\bullet}$ – the donor species – and a pair of oxygen and gallium vacancies $(V_O,V_{Ga})'$ located at the same site – the acceptor species.[9] Recently, this strong blue emission has been demonstrated to show tuneable peak wavelength as a function of colloidal nanocrystal size[5c] and has been successfully coupled, via resonant energy transfer, to the emission of a suitable organic dye bonded onto the nanocrystal surface, thus realizing the first UV-pumped white-emitting diode based on γ-Ga_2O_3.[5b]

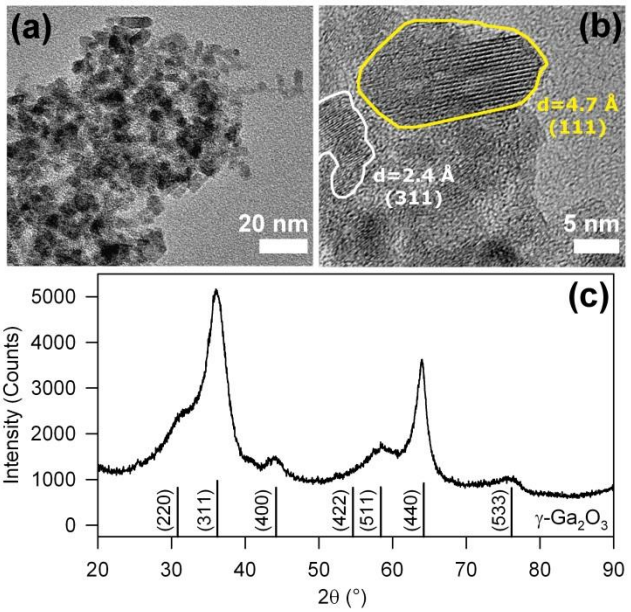

Fig.1 (a) TEM image of the as-synthetized nanopowder. (b) HR-TEM image of one NP shows crystalline features corresponding to lattice parameters of γ-Ga_2O_3 and typically elongated shape parallel to the (111) direction. (c) XRD pattern of as-synthetized NPs, calculated pattern of γ-Ga_2O_3 is reported for comparison.

Here we demonstrate the feasibility of a one-pot non-aqueous solution-based synthesis of rare-earth doped γ-Ga_2O_3 nanosystems with an organic shell. Differently from other syntheses, this approach enriches the spectroscopic features of the nanosystem showing that the crystalline core, the embedded rare-earth dopant ions, and the organic capping resulting from this solvothermal reaction can contribute all together to the light-emission response of the hybrid doped compound. The analysis of the excitation pattern points to the occurrence of mutual excitation mechanisms involving core, shell, and dopant species interactions highlighting the versatility of this material as phosphor with multiple excitation/emission channels.

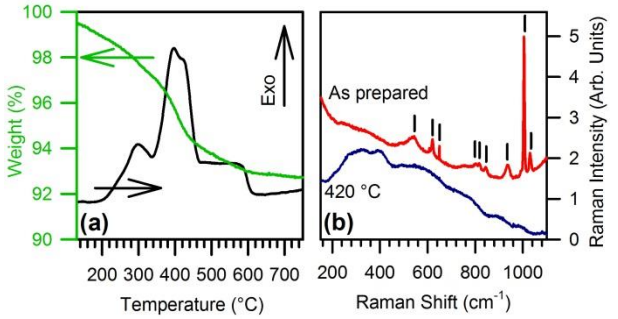

Fig. 2 (a) TGA (green) and DSC (black) curves of as-prepared nanopowder. (b) Raman spectra of as-prepared NPs (red) and after treatment at 420 °C for 1 h (blue), vertical bars indicate peaks ascribed to benzoate.

Nanopowders were prepared by nonaqueous sol-gel chemistry. In a typical synthesis 1 g of gallium (III) acetylacetonate was dissolved in 20 mL of anhydrous benzyl alcohol in a glovebox. For rare earth doped samples, the proper amount of europium acetate was added to the mixture so as to obtain a final doping content of 1% mol_{Eu}/mol_{Ga}. The solution was then poured in a 45 mL PTFE liner and transferred to a steel autoclave (Parr Instrument Company) and accurately sealed. The autoclave was removed from the glovebox and heated in a furnace at 200 °C for 2 days. The resulting milky suspension was washed with diethyl ether, and the obtained precipitate was dried in air at 60 °C for 12 hours.

Representative transmission electron microscopy (TEM) images of nanopowder are reported in Fig. 1a and b. Nanoparticles (NPs) show an elongated shape with preferential growth along the (111) crystal axis (Fig. 1b), with crystal size about 12 nm long and 5 nm wide. The diffraction peaks observed in the XRD pattern of Fig. 1c confirm the formation of γ-Ga_2O_3 (JCPDS 20-0426) and exclude the presence of other crystalline byproducts. The Scherrer analysis of the (440) diffraction peak at 2θ=64° indicates an average crystal size of ~10 nm, in accordance with the TEM outcome. Importantly, TEM and XRD data are significantly different from another non-aqueous sol-gel synthesis of γ-Ga_2O_3 based on benzylamine,[5f] suggesting that the benzyl alcohol route leads to a product with higher crystallinity.

Thermal analysis combined with vibrational spectroscopy reveal the stability and structural features of both core nanocrystals and organic shell. Differential scanning calorimetry and thermal gravimetric analysis (Fig. 2a) evidence a weight loss of about 8% between 200 and 600 °C, concurrent with several exothermal peaks related to the decomposition of organic residuals. Raman analysis before and after a heat treatment in air at 420 °C for 1 h confirms the removal of the organic component. In fact, as prepared powders exhibit narrow Raman peaks (Fig. 2b) at 650, 845, 1010, and 1030 cm^{-1} together with broader modes at 545, 620, 800, 820, and 935 cm^{-1}, which are all consistent with the presence of benzoate groups coordinated to the NPs surface.[10] Heated powders instead show only very broad and weak bands, already ascribed to GaO stretching modes in γ-Ga_2O_3.[3d, 11] The removal of organics seems to be the only effect of the annealing, since the heated NPs show no significant changes in the XRD relative intensities and full width at half maximum (FWHM), this confirms that the metastable γ-phase is preserved after thermal treatment (see ESI).

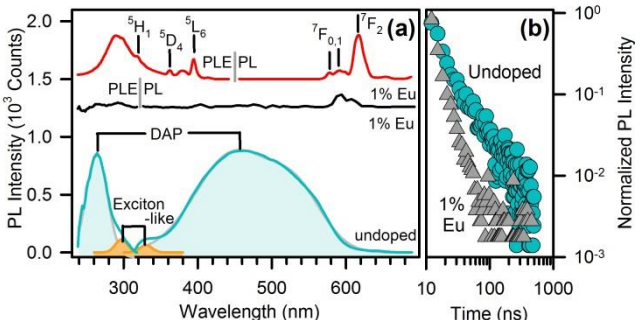

Fig. 3 (a) Photoluminescence (PL) and photoluminescence excitation (PLE) spectra (λ_{EXC}=250 nm, λ_{EMI}= 430 nm) of intrinsic DAPs and exciton-like emission of undoped (blue line) and Eu-doped (black line, shifted up by 1200 counts for clarity) γ-Ga_2O_3 nanoparticles, and PL/PLE spectra (λ_{EXC}=290 nm, λ_{EMI}= 620 nm) of ionic emission in Eu-doped γ-Ga_2O_3 NPs (red line, shifted up by 1500 counts for clarity). (b) Lifetime measurement of doped (grey triangles) and undoped (blue circles) γ-Ga_2O_3 nanoparticles, excited at 250 nm and monitored at 430 nm.

Photoluminescence (PL) and PL excitation (PLE) spectra of undoped and Eu-doped nanopowders without organic capping are reported in Fig. 3a. Emission and excitation patterns of the undoped sample show two distinct emission paths. The most pronounced band is centred in the blue region at 460 nm and arises from DAP recombination excited at 265 nm. A second less intense contribution, centred at 330 nm, is due to exciton-like emission with specific excitation at 300 nm, as already observed in single-crystal gallium oxide[12] as well as in glass/γ-Ga_2O_3 nanocomposites.[13] Spectra taken in the same conditions on Eu doped samples (Fig. 3a, black line) does not show any emission from DAP recombination. Eu related emission is instead dominated by $^5D_0 \rightarrow {}^7F_{0,1,2}$ red emission lines of Eu^{3+} at 570-670 nm (Fig. 3a, red line), excited by the sharp *4f-4f* transitions and within a broad UV excitation at around 290 nm (Fig. 3a). The latter excitation cannot be assigned to intra-centre Eu^{3+} transitions, suggesting energy transfer from the Ga_2O_3 host. The resonance between NPs and Eu^{3+} ions may arise from the overlap between the exciton-like emission of Ga_2O_3 and the *4f-4f* transitions of Eu^{3+}. The broad UV excitation of Eu^{3+} PL is in fact quite similar to the 300 nm exciton-like band of the undoped sample, rather than the DAP band at 265 nm. The occurrence of energy transfer is further confirmed by time resolved PL data: the PL decays of as-synthesized nanopowders (Fig 3b) feature similar stretched exponential kinetics, irrespective of doping, except for a faster decay in presence of Eu^{3+} ions. Assuming a Förster resonance energy transfer (FRET) mechanism governing the emission process, it is possible to evaluate the efficiency E_{FRET} of the NP-Eu^{3+} system from the collected lifetimes.[14] In fact, from the fluorescence lifetime of the donor species – *i.e.* the lifetime of the exciton-like emission of Ga_2O_3 NPs – in presence ($\tau_{D,A}$) and in absence (τ_D) of the acceptor species – *i.e.* the europium ions – the efficiency can be calculated by $E_{FRET}=1-\tau_{D,A}/\tau_D$. Since the kinetics is not a pure single exponential, E_{FRET} is evaluated through the excited state half-life $\tau_{½}$. The experimental values $\tau_{½D,A}$ ~ 2.9 ns and $\tau_{½D}$ ~ 4.0 ns give an E_{FRET} from gallia exciton-like emission to europium of 27%.

On the other hand, when the organic capping is present, *i.e.* before thermal treatment, the full hybrid system shows a

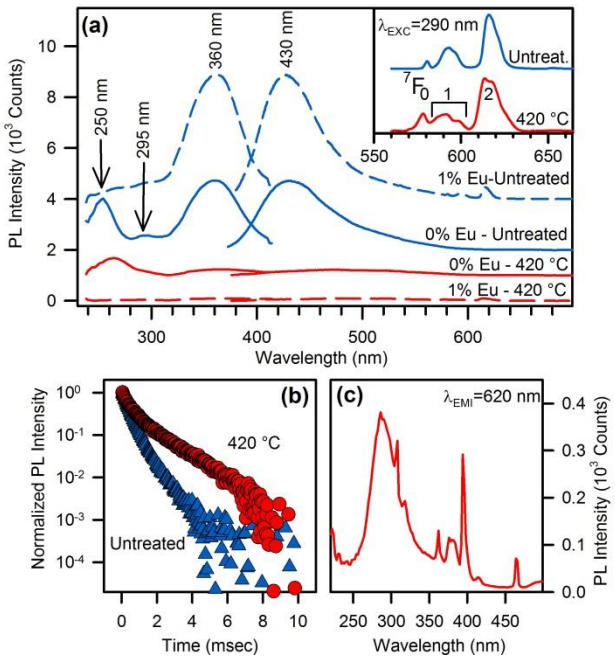

Fig. 4 (a) PL/PLE (λ_{EXC}=340 nm, λ_{EMI}= 430 nm) of undoped (full lines) and Eu-doped (dashed lines) γ-Ga_2O_3 NPs before (blue lines) and after (red lines) organic removal; lines are upshifted by 1000 counts for clarity. Inset: PL (λ_{EXC}=290 nm) of Eu transition of untreated (blue) and treated NPs (red). (b) Lifetime measurements of ionic emission in Eu-doped NPs before (triangles) and after (circles) thermal treatment excited at 250 nm and monitored at 620 nm. (c) Excitation spectra of Eu emission of as-synthetized Eu-doped NPs monitored at 620 nm.

considerable enrichment of the PL and PLE pattern, with additional emission and excitation channels with respect to treated samples. PL and PLE of as-synthesized NPs, irrespective of doping, are dominated by a mirror-like emission with emission and excitation maxima at 430 and 360 nm, respectively (Fig. 4a). This emission is clearly related to the organic shell because of its absence after thermal treatment. However, at least two other spectral features may excite light emission at 430 nm in the full hybrid system, with maxima centred at 295 nm and 250 nm. Since the PLE spectra in Fig. 4a probe the same emission wavelength of the experiments in Fig. 3a, we expect possible contributions arising from nanocrystal excitation spectrum. The shoulder at 295 nm in Fig. 4a can be attributed to exciton-like contribution observed also in treated sample (Fig. 3a). Instead, the broad excitation band at 250 nm deserves some further comments and will be discussed in more detail later.

Besides organic and intrinsic related emission, also Eu^{3+} ion photophysics gives important evidences of the modifications induced by the thermal treatment. As regards Eu^{3+} PL (inset in Fig. 4a), the main changes after thermal treatment at 420 °C are: i) intensity enhancement of the transition $^5D_0 \rightarrow {}^7F_0$ compared with $^5D_0 \rightarrow {}^7F_1$, ii) broadened emissions, and iii) structuring of the spectrum in the $^5D_0 \rightarrow {}^7F_{1,2}$ transition region. These changes are caused by i) a lowering of Eu-O bond distance,[15] ii) a broader distribution of bond length and angles, and iii) the occurrence of Eu ions in more than one preferred site, respectively. The latter conclusion is also supported by lifetime measurements (Fig. 4b). After thermal treatment we observe a considerably slower decay, ascribable to partial suppression of non-radiative decay channels related to organic residuals interacting with Eu^{3+} ions. Furthermore, the curves fitting unveils a biexponential behaviour both in pristine and thermal treated samples (see ESI), but the thermal treatment leads to a smaller relative weight of the fast component and a drastic increase of the slow component lifetime (from 700 μs to 1.5 ms). As evidenced by the presence of extra peaks in the Eu^{3+} emission spectrum, these outcomes confirm that a distinct Eu^{3+} site configuration is introduced by thermally activated structural rearrangement of the host lattice. Additionally, the relative intensity of $^5D_0 \rightarrow {}^7F_2$ and $^5D_0 \rightarrow {}^7F_1$ transitions is a well-known optical probe of the local symmetry of Eu^{3+} ion.[16] Specifically, the absence of inversion symmetry and the lowering of local symmetry cause an enhancement of the first transition with respect to the latter one. The measured ratio (~2.9 both in as-prepared and thermal treated samples) indicates that the local symmetry of Eu^{3+} sites is unaffected by treatment and similar to Eu^{3+} sites in β phase (~2.7).[17] Interestingly, this ratio is instead significantly lower in α- phase (~1.9), whose pure octahedral structure lacks simultaneous occurrence of tetrahedral and octahedral sites, differently from β and γ phases.[18]

Eu-doping also shows clear-cut effects on the excitation pattern of the organic capping, giving a useful tool for clarifying the nature of the organic component. Specifically, we observe that the excitation spectrum of Eu^{3+} monitored at 620 nm shows a strong band corresponding to the exciton-like band at 290 nm, with some minor contributions of comparable intensity in the short- and long-wavelength tails at around 250 nm and 360 nm (Fig. 4c) which disappear after thermal treatment (Fig. 3a). As regard the organic-related blue emission at 430 nm, the presence of Eu ions does not affect the excitation channel at 360 nm, but depresses only the 250 nm excitation band. This band was ascribed to benzoate species attached to the oxide NPs surface.[19] A similar attribution was suggested for the excitation band at 360 nm.[19a, 19b, 20] Following these interpretations, the spectral bands at 250 nm and 360 nm would both belong to the same organic species responsible for the emission at 430 nm. Nevertheless, Eu-doping depresses only one of these two excitation channel. This outcome indirectly points out that the excitation of Eu-related emission does not occur via FRET mechanism. In fact, the Kasha's rule states that light emission from molecules can only occur from the lowest excited state.[14] Accordingly, if the resonant transition responsible for the benzoate-to-Eu^{3+} energy transfer is the 430 nm emission having two PLE structures at 250 and 360 nm which belongs to transitions of the same molecular species, then the presence of Eu^{3+} is necessarily expected to depress both the excitation channels with equal efficiency, contrary to experimental data of Fig. 4a. Indeed, the main excitations of benzyl rings lie in the 200-250 nm region with emission in the 300-350 and 360-450 nm region for fluorescence and phosphorescence, respectively, even in presence of the carbonyl group.[21] Accordingly, benzoate is unlikely responsible for the main excitation channel registered at 360 nm. Moreover, other recent studies on benzoate-enhanced emission of yttrium oxides, in which the occurrence of other contaminants can be excluded,[19] show that PL can be only excited in the 250 nm spectral region, as expected for benzoate species, leading only to near UV fluorescence. Therefore, the presence of an additional organic component other than benzoate must be taken into account in the photophysics of the system, even if it is the main constituent of the organic capping layer as confirmed by Raman, IR and ^{14}C-NMR identification.[10a, 20, 23]

As a consequence, our data in Fig. 4 evidence a more complex system, in which benzoate ligands occur together with an additional organic species responsible for the strong luminescence peak at 430 nm and excited at 360 nm. As a matter of fact, it was already reported the formation of several minor side products resulting from benzyl alcohol route including ketones,[23] hence the presence of molecules like aromatic alpha ketones cannot be excluded. On the other hand, aromatic alpha ketones like benzophenone, acetophenone, and propiophenone, typically possess spectroscopic signature compatible with our experimental evidences and PL quantum yield close to unity.[21a] Furthermore, the Raman spectrum of benzophenone,[10b] for instance, does not present relevant differences with respect to the species found in the capping layer. Consequently, the observed spectroscopy could be tentatively explained by the presence of such aromatic ketones even in small quantity.

As discussed previously, the energy transfer to Eu^{3+} ions occur through resonant Ga_2O_3 NP luminescence (Fig. 3) in the UV rather than through resonance with the DAP blue emission. In a similar way, the organic sensitized emission in untreated NPs involves the preferential coupling with the Eu^{3+} transitions with the UV $\pi \rightarrow \pi^*$ emission of benzoate species, whereas the energy transfer from ketone-related $n \rightarrow \pi^*$ blue emission is much less efficient.

In conclusion, we presented the synthesis of Eu-doped and undoped γ-Ga_2O_3 hybrid nanoparticles with an organic capping resulting from the nonaqueous process. The photophysics of NPs evidences the role of intrinsic and organic-related activation of Eu^{3+} PL. Importantly, the results point out that the presence of negligible amount of organic residuals other than benzoate can be responsible for important optical features due to high PL efficiency.

The authors acknowledge the financial support by ETH of Zürich, the Russian Federation under grant no. 11.G34.31.0027 and by grant MK-1398.2014.3, and Cariplo Foundation, Italy, under project no. 2012-0920. M.J. Süess and ScopeM – ETH Zürich are gratefully acknowledged for TEM imaging.

Notes and references

[a]Department of Materials Science, University of Milano-Bicocca, via R. Cozzi 55, I-20125 Milano, Italy.

E-mail: roberto.lorenzi@mater.unimib.it

[b]P.D. Sarkisov International Laboratory of Glass-Based Functional Materials, Mendeleyev University of Chemical Technology of Russia, Miusskaya Square 9, 125047 Moscow, Russia.

[c]Department of Materials, ETH Zürich, Vladimir-Prelog-Weg 5 - 8093 Zurich, Switzerland.

E-mail: alessandro.lauria@mat.ethz.ch

Electronic Supplementary Information (ESI) available: materials & method, XRD patterns and fitting results on lifetime measuremet. See DOI: 10.1039/c000000x/

1(a) E. Nogales, B. Méndez, J. Piqueras and J. A. García, *Nanotechnology*, 2009, **20**, 115201; (b) M. L. Pang, W. Y. Shen and J. Lin, *Journal of Applied Physics*, 2005, **97**.

2 J. C. Le Breton, H. Saito, S. Yuasa and K. Ando, *Applied Physics Letters*, 2009, **94**.

3(a) X. Wang, Q. Xu, M. Li, S. Shen, X. Wang, Y. Wang, Z. Feng, J. Shi, H. Han and C. Li, *Angewandte Chemie International Edition*, 2012, **51**, 13089; (b) S. Arnold, S. Prokes, F. Perkins and M. Zaghloul, *Applied Physics Letters*, 2009, **95**, 103102; (c) Z. Liu, T. Yamazaki, Y. Shen, T. Kikuta, N. Nakatani and Y. Li, *Sensors and Actuators B: Chemical*, 2008, **129**, 666; (d) Y. Hou, L. Wu, X. Wang, Z. Ding, Z. Li and X. Fu, *Journal of Catalysis*, 2007, **250**, 12; (e) Y. Hou, X. Wang, L. Wu, Z. Ding and X. Fu, *Environmental science & technology*, 2006, **40**, 5799.

4(a) S. Yoshioka, H. Hayashi, A. Kuwabara, F. Oba, K. Matsunaga and I. Tanaka, *Journal of Physics: Condensed Matter*, 2007, **19**, 346211; (b) R. Roy, V. Hill and E. Osborn, *Journal of the American Chemical Society*, 1952, **74**, 719.

5(a) T. Wang, A. Layek, I. D. Hosein, V. Chirmanov and P. V. Radovanovic, *Journal of Materials Chemistry C*, 2014; (b) T. Wang, V. Chirmanov, W. H. M. Chiu and P. V. Radovanovic, *Journal of the American Chemical Society*, 2013, **135**, 14520; (c) M. Hegde, T. Wang, Z. L. Miskovic and P. V. Radovanovic, *Applied Physics Letters*, 2012, **100**, 141903; (d) T. Wang and P. V. Radovanovic, *The Journal of Physical Chemistry C*, 2011, **115**, 18473; (e) T. Wang, S. S. Farvid, M. Abulikemu and P. V. Radovanovic, *Journal of the American Chemical Society*, 2010, **132**, 9250; (f) N. Pinna, G. Garnweitner, M. Antonietti and M. Niederberger, *Journal of the American Chemical Society*, 2005, **127**, 5608.

6 H. Hayashi, R. Huang, F. Oba, T. Hirayama and I. Tanaka, *Journal of Materials Research*, 2011, **26**, 578.

7 D. Kisailus, Q. Truong, Y. Amemiya, J. C. Weaver and D. E. Morse, *Proceedings of the National Academy of Sciences*, 2006, **103**, 5652.

8 V. N. Sigaev, N. V. Golubev, E. S. Ignat'eva, B. Champagnon, D. Vouagner, E. Nardou, R. Lorenzi and A. Paleari, *Nanoscale*, 2013, **5**, 299.

9 L. Binet and D. Gourier, *Journal of Physics and Chemistry of Solids*, 1998, **59**, 1241.

10(a) A. Lauria, I. Villa, M. Fasoli, M. Niederberger and A. Vedda, *Acs Nano*, 2013, **7**, 7041; (b) B. Schrader, *Raman/infrared atlas of organic compounds*, VCH, Weinheim, 1989.

11 H. Seshadri, P. Sasidhar and P. Sinha, *International Journal of Environment and Waste Management*, 2013, **11**, 244.

12 K. Shimamura, E. G. Víllora, T. Ujiie and K. Aoki, *Applied Physics Letters*, 2008, **92**, 201914.

13(a) V. N. Sigaev, N. V. Golubev, E. S. Ignat'eva, A. Paleari and R. Lorenzi, *Nanoscale*, 2014, **6**, 1763; (b) Z. Liu, X. Jing and L. Wang, *Journal of The Electrochemical Society*, 2007, **154**, H440; (c) G. Blasse and A. Bril, *Journal of Physics and Chemistry of Solids*, 1970, **31**, 707.

14 J. Lakowicz, *Principles of Fluorescence Spectroscopy*,Springer, New York, 3rd ed., 2006.

15 H. You and M. Nogami, *The Journal of Physical Chemistry B*, 2004, **108**, 12003.

16 E. Zych, *Journal of Physics: Condensed Matter*, 2002, **14**, 5637.

17 H. Xie, L. Chen, Y. Liu and K. Huang, *Solid state communications*, 2007, **141**, 12.

18(a) J. Ahman, G. Svensson and J. Albertsson, *Acta Crystallographica Section C: Crystal Structure Communications*, 1996, **52**, 1336; (b) H. Y. Playford, A. C. Hannon, M. G. Tucker, D. M. Dawson, S. E. Ashbrook, R. J. Kastiban, J. Sloan and R. I. Walton, *The Journal of Physical Chemistry C*, 2014, **118**, 16188.

19(a) M. Karmaoui, R. A. Sá Ferreira, A. T. Mane, L. D. Carlos and N. Pinna, *Chemistry of materials*, 2006, **18**, 4493; (b) R. A. Sá Ferreira, M. Karmaoui, S. S. Nobre, L. D. Carlos and N. Pinna, *Chemphyschem*, 2006, **7**, 2215; (c) N. Pinna, G. Garnweitner, P. Beato, M. Niederberger and M. Antonietti, *Small*, 2005, **1**, 112.

20 X. Bai, A. Pucci, V. T. Freitas, R. A. Ferreira and N. Pinna, *Advanced functional materials*, 2012, **22**, 4275.

21(a) M. Montalti, A. Credi, L. Prodi and M. T. Gandolfi, *Handbook of photochemistry*, CRC press, 2006; (b) S. P. McGlynn, T. Azumi and D. Kumar, *Chemical Reviews*, 1981, **81**, 475; (c) R. Martin and G. A. Clarke, *Journal of Physical Chemistry*, 1978, **82**, 81; (d) H. Baba and M. Kitamura, *Journal of Molecular Spectroscopy*, 1972, **41**, 302; (e) H. J. Maria and S. P. McGlynn, *Journal of Chemical Physics*, 1970, **52**, 3399.

22 X.-L. Liu, P.-X. Zhu, Y.-F. Gao and R.-H. Jin, *Journal of Materials Chemistry C*, 2013, **1**, 477.

23 M. Niederberger, G. Garnweitner, N. Pinna and M. Antonietti, *Journal of the American Chemical Society*, 2004, **126**, 9120.

